NASA TECHNICAL NOTE

VIBRATIONAL RELAXATION AND RADIATIVE GAIN IN EXPANDING FLOWS OF ANHARMONIC OSCILLATORS

by Robert L. McKenzie

Ames Research Center
Moffett Field, Calif. 94035

NATIONAL AERONAUTICS AND SPACE ADMINISTRATION • WASHINGTON, D. C. • MARCH 1971

1. Report No. NASA TN D-7050	2. Government Accession No.	3. Recipient's Catalog No.
4. Title and Subtitle VIBRATIONAL RELAXATION AND RADIATIVE GAIN IN EXPANDING FLOWS OF ANHARMONIC OSCILLATORS		5. Report Date March 1971 6. Performing Organization Code
7. Author(s) Robert L. McKenzie		8. Performing Organization Report No. A-3789 10. Work Unit No. 129-01-22-01-00-21
9. Performing Organization Name and Address NASA Ames Research Center Moffett Field, Calif., 94035		11. Contract or Grant No. 13. Type of Report and Period Covered Technical Note
12. Sponsoring Agency Name and Address National Aeronautics and Space Administration Washington, D. C. 20546		14. Sponsoring Agency Code
15. Supplementary Notes		

16. Abstract

The set of master rate equations for the vibrational relaxation of mixtures of anharmonic diatomic gases in supersonic nozzle expansions is integrated numerically. Large deviations from a Boltzmann distribution of vibrational state population are predicted, particularly when vibrational energy is exchanged between two near-resonant diatomic species. Radiative gain coefficients for nonequilibrium vibration-rotation transitions are also computed and positive gains, sufficient to support laser oscillations, are predicted for CO-N_2 and CO-N_2-Ar admixtures.

17. Key Words (Suggested by Author(s)) Vibrational relaxation Vibrationally relaxing flows Gas dynamic laser Carbon monoxide Anharmonic oscillator relaxation	18. Distribution Statement Unclassified – Unlimited		
19. Security Classif. (of this report) Unclassified	20. Security Classif. (of this page) Unclassified	21. No. of Pages 26	22. Price* $3.00

*For sale by the National Technical Information Service, Springfield, Virginia 22151

VIBRATIONAL RELAXATION AND RADIATIVE GAIN IN EXPANDING FLOWS OF ANHARMONIC OSCILLATORS

Robert L. McKenzie

Ames Research Center

SUMMARY

The equations governing the vibrational relaxation of anharmonic oscillators in mixtures comprised of several oscillator species have been solved numerically for supersonic nozzle expansions. The master equations, describing the rate of population change in each vibrational level of each species considered, include terms accounting for vibration-to-translation (V-T) and vibrational-to-vibration (V-V) energy transfer. A method of truncating the set of equations is developed to reduce the required number of equations while maintaining an accurate solution for those retained. The solutions are obtained by the use of an implicit integration scheme with the dependent variables represented by a set of non-Boltzmann distribution parameters. The resulting population distributions among the vibrational states are found to display no obvious, low-order, polynomial form when large deviations from a Boltzmann population distribution are predicted. Significant overpopulations of the upper vibrational levels are predicted for expanding flows.

The associated radiative gain coefficients are also computed for the infrared vibration-rotation bands of CO. They are found to be strongly influenced by the effects of anharmonic energy states on the relaxation process. Radiative features are sensitive mainly to the magnitude of the V-V transition probabilities and their variation with vibrational quantum number. The radiative gain predictions in expanding flows of CO or CO-N_2-Ar are found to be of sufficient magnitude to support high-power laser oscillation through strictly gasdynamic means, even in view of the uncertainties in vibrational relaxation rates for expanding flows.

INTRODUCTION

Until recently, vibrational relaxation in flowing gases was usually analyzed by adopting a harmonic oscillator model of the quantized vibrational energy states (ref. 1). The simple Landau-Teller dependence of transition probabilities on vibrational quantum number, along with the prior knowledge that a Boltzmann population of harmonic states will persist, then allowed the set of rate equations to be combined into a single expression for the rate of change of average vibrational energy. The model was commonly restricted further by considering only the transfer of energy between vibrational and translational modes. To verify the Landau-Teller theory, measurements were usually made at conditions where either vibrational excitation predominated

(shock-wave experiments) or where only small departures from equilibrium existed (ultrasonic experiments). For those circumstances, the harmonic oscillator model provided an adequate description of the experimental results.

Recently, however, vibrational de-excitation experiments in expanding flows (refs. 2, 3) have yielded seemingly large discrepancies between relaxation rates inferred from a harmonic oscillator analysis of the expansion process and the rates obtained from shock-wave experiments. Those results stimulated further examination of the oscillator model and led to new investigations of the effects caused by small anharmonic terms in the oscillator potential.

Treanor, Rich, and Rehm (ref. 4) provided a recent comprehensive analysis of vibrational relaxation among anharmonic oscillators, and used a "zeroth-order" approximation to show that the small anharmonicity of common diatomic gases can significantly enhance the relaxation of lower vibrational levels in a rapid de-excitation process. Later, Bray (ref. 5) used a first-moment method to obtain approximate solutions to the complete set of rate equations and demonstrated the manner in which upper level non-Boltzmann distributions develop among anharmonic nitrogen-like oscillators.

Those recent studies (refs. 4, 5) are primarily qualitative, however, and apply to generalized nonequilibrium situations. Their limitations are necessary because both studies rely on some form of analytical approximation for solving the nonlinear differential rate equations. The work described in this paper was therefore undertaken to explore the results of more complete numerical solutions that not only provide a basis for evaluating the previous analytical approximations but, more importantly, allow some additional details regarding the effects of practical gasdynamic conditions to be conveniently included. Here, the rate equations for arbitrary mixtures of monatomic and anharmonic diatomic gases have been numerically integrated along the axes of quasi-one-dimensional supersonic nozzle expansions. The corresponding nonequilibrium radiative properties are also obtained since most experimental methods for determining the nonequilibrium state of a gas rely on its radiative properties. Furthermore, the non-Boltzmann characteristics of vibrational energy level populations in nonequilibrium expansions suggest several applications to gas laser devices.

ANALYTICAL MODEL

Treanor, Rich and Rehm (ref. 4) have shown that the population distribution among the lower levels of vibrationally relaxing anharmonic oscillators approaches the form

$$N_j^v = N_j^o \exp\left(\alpha v - \frac{E_j^v}{kT}\right) \tag{1}$$

where N_j^v is the number density of species j in vibrational state v, E_j^v is the energy above the ground state, T is the kinetic temperature, and α is a time-dependent nonequilibrium factor, independent of species or vibrational quantum number. In rapidly cooled flows, where E_j^v/kT greatly exceeds unity, αv can reach values nearly equal to E_j^v/kT, leaving the small nonlinear anharmonic terms in E_j^v to describe a significantly non-Boltzmann distribution via equation (1).

From the above, a tempting approximation for the anharmonic model is to assume distributions in the form of equation (1), and reduce the set of rate equations to a single expression for $d\alpha(t)/dt$, or some other suitable parameter. The solutions to follow will show, however, that in many cases of interest, α varies enough with v to make such an approximation unsatisfactory for other than the lowest energy levels. In this analysis, the population fractions of each vibrational state are treated as separate dependent variables. The set of coupled, nonlinear differential equations describing the rate of change of each variable is then numerically integrated along the axis of an arbitrarily defined one-dimensional flow. No restrictions are placed on the distribution of oscillators among vibrational energy states other than to conserve their total number. Vibrational transitions are limited to single quantum jumps, however, since multiquantum transition probabilities are generally insignificant at the temperatures of present interest (ref. 6). The populations of all rotational states are assumed to remain in thermodynamic equilibrium with the local translational temperature of the gas, and vibrational energy is allowed to be transferred only through collisions. (Spontaneous radiative transitions, which become important at very low pressures or for very high-lying vibrational states, are omitted.) Finally, only supersonic expanding flows are considered. In those cases, expansion rates which far exceed the collisional rates of vibrational de-excitation are easily obtained, and changes in the average vibrational energy of all oscillators remain small during the expansion, contributing little to the fluid thermodynamics. The flow properties may then be conveniently uncoupled from the vibrational relaxation process and the local thermodynamic state of the gas computed using well-known perfect gas equations for a constant isentropic exponent.

The Rate Equations

The number density of oscillators, N_j^v, of species j in vibrational quantum state v may be written in terms of a mole fraction, X_j^v, relative to the entire gas mixture,

$$X_j^v = \frac{N_j^v}{\sum_{j,v} N_j^v} \tag{2}$$

In general terms, the temporal rate of change of X_j^v due to a collisional relaxation process may then be written

$$\frac{dX_j^v}{dt} = \sum_k Z_{jk} Q_{jk}^v \tag{3}$$

where Q_{jk}^v is the molar production per collision of X_j^v due to encounters between species j and k, and Z_{jk} is an average collision rate given by

$$Z_{jk} = \frac{\rho}{m} d_{jk}^2 \sqrt{\frac{8\pi kT}{\mu_{jk}}} \tag{4}$$

In equation (4), ρ and m are the average fluid density and molecular weight, d_{jk}^2 is an averaged collision cross section for encounters between species j and k, and μ_{jk} is their reduced mass. If the total mole fraction of species k is denoted as $\hat{X}_k = \sum_L X_k^L$, including all vibrational quantum states L, and only single quantum transitions are considered, the vibration-to-translation (V - T) energy exchange contributes

$$[Q_{jk}^v]_{V-T} = \hat{X}_k P_{jk}^{1,0} \left\{ \overline{P}_{jk}^{v,v-1} \left[X_j^{v-1} \exp\left(\frac{-E_j^{v,v-1}}{kT} \right) - X_j^v \right] + \overline{P}_{jk}^{v+1,v} \left[X_j^{v+1} - X_j^v \exp\left(\frac{-E_j^{v+1,v}}{kT} \right) \right] \right\} \tag{5a}$$

while the vibration-to-vibration (V - V) energy transfer contributes

$$\left[Q_{jk}^v \right]_{V-V} = P_{jk}\binom{0,1}{1,0} \sum_L \left\{ \overline{P}_{jk}\binom{L,L+1}{v,v-1} \left[X_j^{v-1} X_k^{L+1} \exp\left(\frac{E_k^{L+1,L}}{kT} - \frac{E_j^{v,v-1}}{kT} \right) - X_j^v X_k^L \right] + \overline{P}_{jk}\binom{L,L+1}{v+1,v} \left[X_j^{v+1} X_k^L - X_j^v X_k^{L+1} \exp\left(\frac{E_k^{L+1,L}}{kT} - \frac{E_j^{v+1,v}}{kT} \right) \right] \right\} \tag{5b}$$

The total production term is then

$$Q_{jk}^v = \left[Q_{jk}^v \right]_{V-T} + \left[Q_{jk}^v \right]_{V-V} \tag{5c}$$

Equations (5) include the detailed balance relations, exemplified by

$$P_{jk}^{v-1,v} = P_{jk}^{v,v-1} \exp\left(\frac{-E_j^{v,v-1}}{kT}\right)$$

and are written in terms of relative transition probabilities

$$\left.\begin{aligned} \overline{P}_{jk}^{r,s} &= \frac{P_{jk}^{r,s}}{P_{jk}^{1,0}} \\ \overline{P}_{jk}\binom{\ell,m}{r,s} &= \frac{P_{jk}\binom{\ell,m}{r,s}}{P_{jk}\binom{1,0}{0,1}} \end{aligned}\right\} \tag{6}$$

In the notation above, $P_{jk}^{r,s}$ is the V - T probability per collision that species j will make the transition from vibrational quantum state r to s as a result of an encounter with species k. Similarly, $P_{jk}\binom{\ell,m}{r,s}$ is the V - V probability per collision that an encounter between species j and k will cause an r to s transition in species j and a simultaneous ℓ to m transition in species k.

Terms similar to $E_j^{v,v-1}$ in equations (5) are the energy difference between two adjacent states, v and v - 1, of species j. They may be evaluated by assuming a Morse oscillator model in which the vibrational energy above the ground state is given by

$$E_j^v = k\theta_j v[1 - \varepsilon_j(v + 1)] \tag{7a}$$

Here, θ_j is a characteristic oscillator temperature and ε_j is the small anharmonic coefficient (see table 1).

TABLE 1.- TRANSITION PROBABILITY CONSTANTS

Species	θ_j, °K	ε_j	d_j^2, cm^2
CO	3122	6.203×10^{-3}	1.36×10^{-15}
N_2	3395	6.217×10^{-3}	1.38×10^{-15}
Ar	---	---	6.75×10^{-16}

The energy difference, $E_j^{v,v-1}$ is then

$$E_j^{v,v-1} = k\theta_j(1 - 2\varepsilon_j v) \tag{7b}$$

Transition Probabilities

The dependence of both the V - T and V - V transition probabilities on vibrational quantum number continues to be one of the largest uncertainties in existing theoretical models.. For that reason, we shall not belabor the accuracy of the probability ratios $\overline{P}_{jk}$ used in this study but, instead, explore the consequences of their uncertainties on the relaxation process. As Bray (ref. 5) shows, a convenient form of the theory of Schwartz, Slawsky, and Herzfeld (ref. 7) can be adopted in which the probability ratios are given by

$$\overline{P}_{jk}^{v,v-1} = v\left(\frac{1 - \varepsilon_j}{1 - v\varepsilon_j}\right)\frac{F_j^v}{F_j^1} \tag{8a}$$

$$\overline{P}_{jk}\binom{L,L+1}{v,v-1} = v(L + 1)\left(\frac{1 - \varepsilon_j}{1 - v\varepsilon_j}\right)\left(\frac{1 - \varepsilon_k}{1 - L\varepsilon_k}\right)\frac{F_{jk}^{v,L}}{F_{jk}^{1,0}} \tag{8b}$$

The integral expressions of the adiabaticity factors F_j^v and $F_{jk}^{v,L}$ are evaluated by an empirical fit of Keck and Carrier (ref. 8) which conveniently bridges the gap between impulsive and adiabatic energy exchange. Keck and Carrier suggested the form

$$F = \frac{1}{2}\left(3 - e^{-K\lambda}\right)e^{-K\lambda} \tag{9}$$

and obtained the best fit for $K = 2/3$. In this application, $K = 2/3$ is used as a nominal value but is also retained as an uncertain parameter. In equation (9), λ is given by

$$\lambda_{jk} = \frac{2\pi^2 \ell_{jk}}{h}\sqrt{\frac{\mu_{jk}}{2kT}}\ |\Delta E_{jk}| \tag{10}$$

where ℓ_{jk} is a range parameter describing the intermolecular potential and has been set equal to 0.2 Å in all cases here. The magnitude of the net vibrational energy difference for the V - T or V - V exchange in question is denoted by $|\Delta E_{jk}|$. The variation of $\overline{P}$ with v based on equations (8) to (10) and the parameters for CO from table 1 is shown in figure 1. A comparison of the harmonic and Morse oscillator curves clearly shows that the small anharmonic coefficient, ε_j, has a large effect on the transition probability predictions.

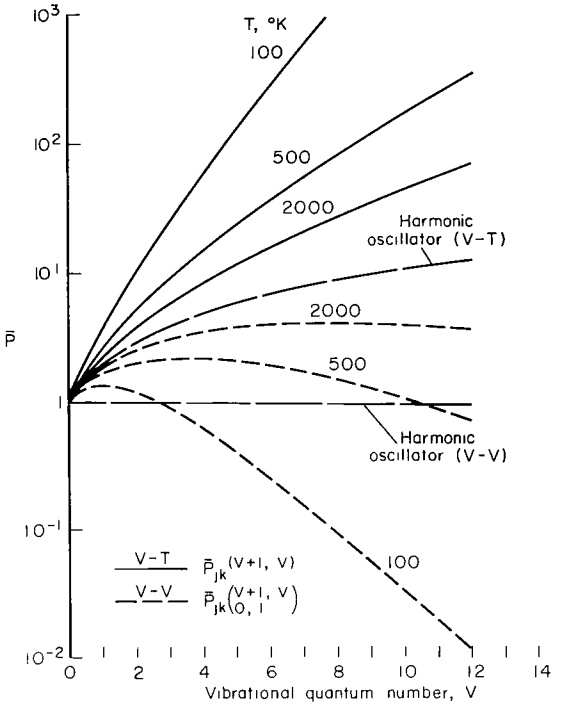

Figure 1.— Normalized transition probabilities for harmonic and anharmonic CO.

Equation (5) also requires absolute values of the ground state probabilities, $P_{jk}^{1,0}$ and $P_{jk}\binom{0,1}{1,0}$. Since, in many cases, existing theories do not successfully reproduce the absolute magnitudes of the experimental results, preference is given here to an empirical formulation of the experimental values. Data are available, at least for the $P_{jk}^{1,0}$ values, because they are the most easily obtained from measurements of the net relaxation time τ_{jk}. Under the conditions of shock wave experiments, τ_{jk} depends principally on $P_{jk}^{1,0}$, and may be correlated in the form

$$\tau_{jk} = \frac{B_{jk}}{p} \exp\left(C_{jk} T^{-1/3}\right) \qquad (11)$$

It is related to $P_{jk}^{1,0}$ by

$$P_{jk}^{1,0} = \left[\tau_{jk} p d_{jk}^2 \hat{X}_k \sqrt{\frac{8\pi}{\mu_{jk} kT}} \left(1 - e^{-\theta_j/T}\right)\right]^{-1} \qquad (12)$$

Values of B_{jk} and C_{jk} used in this study were determined from the data of references 9 and 10.

Experimental data for the V - V probability $P_{jk}\binom{0,1}{1,0}$ are more difficult to obtain. However, what little is available and useful for this work (e.g., refs. 11 and 12) shows that convenient closed-form expressions like those from reference 7 are usually suitable for predicting the temperature dependence of $P_{jk}\binom{0,1}{1,0}$ but must often be adjusted in magnitude. Nominal values of $P_{jk}\binom{0,1}{1,0}$ are obtained here from the following: Schwartz, Slawsky, and Herzfeld (ref. 7) described the transition probabilities for V - V transfer between energy levels far from resonance as

$$P_{jk}\binom{0,1}{1,0} = 0.39\,\pi^2 \frac{\mu_{jk}^2}{M_j M_k} \frac{(\Delta E_{jk})^2}{E_j^1 E_k^1} \frac{\sigma_{jk}^{3/2} e^{-\sigma_{jk}}}{1 - e^{-(2/3)\sigma_{jk}}} \qquad (13a)$$

where

$$\sigma_{jk} = 3\left[\frac{2\pi^4 \mu_{jk} \ell_{jk} (\Delta E_{jk})^2}{h^2 kT}\right]^{1/3} - \frac{\Delta E_{jk}}{2kT} \tag{13b}$$

and

$$\Delta E_{jk} = \left| E_j^1 - E_k^1 \right|$$

In equations (13), M_j is the reduced mass of the oscillator j and E_j^1 is its energy given by equations (7) for v = 1. For the near-resonant case, Treanor (ref. 13) reported a modified version of the theory in reference 7 for small energy differences which reduces to the theory of reference 7 for exact resonance; namely,

$$P_{jk}\binom{0,1}{1,0} = \frac{\mu_{jk} h^2 kT \, e^{-\Omega_{jk}}}{4\pi^2 M_j M_k \ell_{jk}^2 E_j^1 E_k^1} \tag{14a}$$

where

$$\Omega_{jk} = \frac{8\pi^4}{25} \ell_{jk}^2 \mu_{jk} \frac{(\Delta E_{jk})^2}{h^2 kT} \tag{14b}$$

As Treanor (ref. 13) pointed out, when either equations (13) or (14) are used away from the region in which they apply, the prediction is too small. Hence, the larger of the results is used in this work.

Truncation Methods

With the preceding equations, all the terms of equation (3) are specified and the set of rate equations - one for each species j and each energy state v - can be written. Since chemical reactions are excluded, the set of equations can be reduced by one for each species by including the conservation condition:

$$\hat{X}_j = \sum_v X_j^v = \text{constant} \tag{15}$$

The number of remaining equations is still excessive, however, since most oscillators of interest contain about 50 vibrational states below the dissociation energy limit. Fortunately, if our interest is only in the lower levels, we can note that only negligible energy transfer occurs between the upper levels near the dissociation limit and those near the ground state. For many cases of practical interest, however, experience has shown that at least

20 levels must be retained to preserve accuracy in the total number of oscillators available. For example, if all but say the first 10 levels are excluded, an overpopulation of levels above the tenth could demand a large fraction of the available oscillators. Equation (15), summed only over the first 10 levels would then introduce large errors. However, even cases with 20 levels and a single species require excessive computing times, making multiple-species calculations impractical. To minimize the total number of equations while maintaining sufficient accuracy, advantage can be taken of the behavior of the upper levels which couple principally through the conservation of oscillators expressed by equation (15). Collisional-energy-transfer coupling between nearby levels, through equations (3) to (5), was found to be negligible beyond the nearest 2 or 3 states. Hence, little is compromised in the accuracy of the populations of the lower levels by properly substituting a partition function in equation (15) to account for those levels above the last one desired in the numerical integration. The rate equations are then truncated to a reasonable number (say 10 or less for each species) and only the population of the last few quantum states may be expected to contain some error. The definition of an upper level partition function requires some knowledge of the population distributions of those states for the anharmonic oscillators. The results are not too sensitive to the crudeness of the estimate, however, and a satisfactory method is to define a "vibrational temperature" based on the relative populations of the ground state and the last state included in the integration. If we denote the quantum number of the last vibrational state included as $\bar{v}$, a vibrational temperature may be defined by

$$T_j^{\bar{v}} = \frac{E_j^{\bar{v}}}{k \ \ell n \left(\frac{X_j^{\bar{v}}}{X_j^o} \right)} \tag{16}$$

A Boltzmann distribution, described by $T_j^{\bar{v}}$ is then assumed for all states between $\bar{v}$ and the dissociation-limited last state with quantum number v_d. Equation (15) can be replaced by

$$\hat{X}_j = X_j^o \left[1 + \sum_{v=1}^{\bar{v}} \frac{X_j^v}{X_j^o} + \sum_{v=\bar{v}+1}^{v_d} \exp \left(- \frac{E_j^v}{k T_j^{\bar{v}}} \right) \right] \tag{17}$$

By approximating the values of E_j^v in the second summation with $E_j^v = k\theta_j v$, we can obtain the numerically convenient form

$$\hat{X}_j = X_j^o \left(1 + \sum_{v=1}^{\bar{v}} \frac{X_j^v}{X_j^o} + \frac{e^{-\theta_j \bar{v}/T_j^{\bar{v}}} - e^{-\theta_j v_d/T_j^{\bar{v}}}}{e^{\theta_j/T_j^{\bar{v}}} - 1} \right) \tag{18}$$

Numerical experiments with the use of equation (18) showed that in the expanding flows of interest, truncation to as few as five levels still reproduced the fourth level populations within 15 percent and had only a negligible effect on the ground state values. Five-level solutions without the partition function term in equation (18) had little similarity to more exact results. Some large errors still remained in the population of states near $\bar{v}$, however, for cases with developing population inversions. The inversions become artificially enhanced by the truncation, starting at three or four levels below $\bar{v}$. The difficulty was caused by a restriction in the rate equations which forbid transitions between oscillators in the $\bar{v}$ state and the next higher level. Such a restriction is a natural consequence of equation (15) whose differentiation leads to

$$\frac{d\hat{X}_j}{dt} = \sum_k \sum_{v=0}^{\bar{v}} Z_{jk} Q_{jk}^{v} = 0 \qquad (19)$$

The combined use of equations (15) and (19) is referred to here as a "full truncation." The addition of $\bar{v} \rightleftarrows \bar{v} + 1$ transitions violates the condition of equation (19) only slightly for $\bar{v} > 10$, and reduces the errors in X_j^v near $v = \bar{v}$ considerably. Species conservation is retained by continuing the use of equation (15). Hence, removal of the restriction given by equation (19) is an essential aspect of the truncation method and is referred to here as a "partial truncation," since equation (15) is retained but not its derivative.

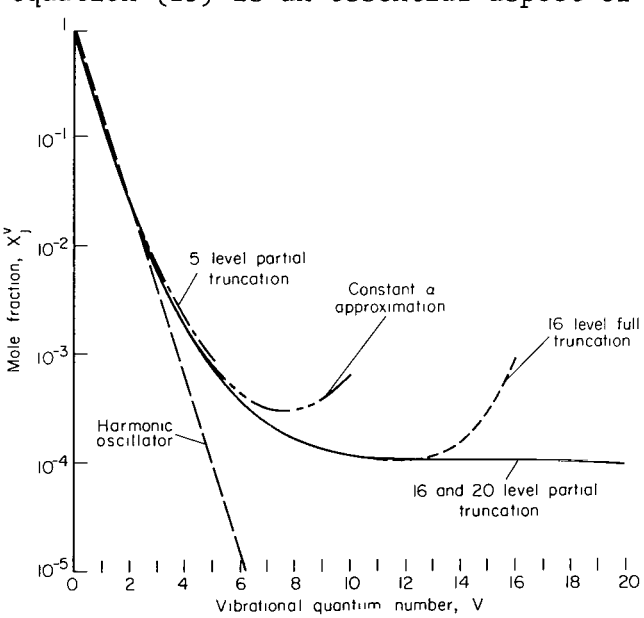

Figure 2.— Truncation effects. (Flow conditions are defined by the standard case described in the text. The data pertain to CO at $A/A_* = 200$.)

The effects of these truncation methods are illustrated in figure 2 for a typical solution. The 16-level, partially truncated model clearly reproduces a more accurate 20-level model with only negligible errors, while the fully truncated 16-level model displays an artificial inversion. The 5-level, partially truncated, model also maintains acceptable accuracy and was obtained in 1/30 of the computation time required by the 20-level version. Although these methods appear successful in the applications shown here, their validity should be retested for other situations.

METHOD OF SOLUTION

The successful application of many numerical integration schemes is often aided by the selection of dependent variables that all maintain similar magnitudes near unity. Such variables are usually difficult to find, especially in chemical nonequilibrium problems where species concentrations vary by many orders of magnitude. Here, however, advantage can be taken of the nature of the solution which approaches the form given by equation (1) for the lower levels. The parameter α has only a weak dependence on species or quantum state and, for typical expansion cases, ranges through positive values within a few orders of unity. The α parameter therefore serves as a much more favorable dependent variable than X_j^v, since the latter varies with v and time by many orders of magnitude. From equation (1), a convenient transformation is

$$\alpha_j^v = \frac{1}{v}\left[\frac{E_j^v}{kT} + \ell n\left(\frac{X_j^v}{X_j^o}\right)\right] \tag{20}$$

which allows equation (3) to be recast in terms of α_j^v. For this application, the one-dimensional flow axial coordinate y shall be adopted as the independent variable via $dy = u\,dt$, where u is the local fluid velocity. If Q_j^v is defined by $Q_j^v = dX_j^v/dt = \sum_k Z_{jk}Q_{jk}^v$, equation (3) can then be rewritten for $v \neq 0$ as

$$\frac{d\alpha_j^v}{dy} = \frac{1}{v}\left[\frac{1}{u}\left(\frac{Q_j^v}{X_j^v} - \frac{Q_j^o}{X_j^o}\right) - \frac{E_j^v}{kT^2}\frac{dT}{dy}\right], \qquad v > 0 \tag{21}$$

where X_j^v and X_j^o $(v = 0)$ are computed in terms of α_j^v and $\hat{X}_j$ by inverting equations (18) and (20).

The set of equations (21) (in conjunction with the fluid dynamic variables u, ρ, T, and dT/dy found from isentropic flow equations in terms of the area ratio $A(y)/A_*$) was integrated as a function of y by means of an implicit finite-difference scheme of Lomax and Bailey (ref. 14). Briefly, for this application, the method requires solutions to the linearized matrix equation

$$\left([I] - \frac{\Delta y}{2}[A_n]\right)\left(\vec{W}_{n+1} - \vec{W}_n\right) = \Delta y\vec{F}_n$$

where $[I]$ is a unit matrix and Δy is the step size. The vectors $\vec{W}_n$ and $\vec{F}_n$ are defined at the nth step in transposed form as

$$\vec{W}_n^T = \left(\alpha_j^1,\ \alpha_j^2,\ \ldots,\ \alpha_j^{\bar{v}},\ \ldots,\ \alpha_k^{\bar{v}},\ y\right)$$

$$\vec{F}_n^T = \left(Q_j^1,\ Q_j^2,\ \ldots,\ Q_j^{\bar{v}},\ \ldots,\ Q_k^{\bar{v}},\ 1\right)$$

The matrix $[A_n]$ consists of the elements $A_{ij} = \partial F_i/\partial W_j$ at step n and where found by the numerical differencing procedure applied in reference 14. This method was found to be advantageous because it allowed the successful integration of the set of equations used here without further specialization or development. For comparison, cases computed by either a conventional or modified (ref. 15) fourth-order Runge-Kutta scheme developed extreme oscillations which eventually terminated the solution.

Solution Characteristics

The flow properties controlling the relaxation process are defined in this study by the half-angle and throat height of two-dimensional wedge-shaped nozzles. The starting procedure for the examples to follow assumes an initial value of y corresponding to a station just upstream of the sonic throat and a set of constant α_j^v values corresponding to a lower state vibrational temperature 5 percent greater than the local kinetic temperature. These initial conditions approximate the progress of the relaxation process from the reservoir and have little effect on the downstream conditions. A standard case has been selected with the following general properties:

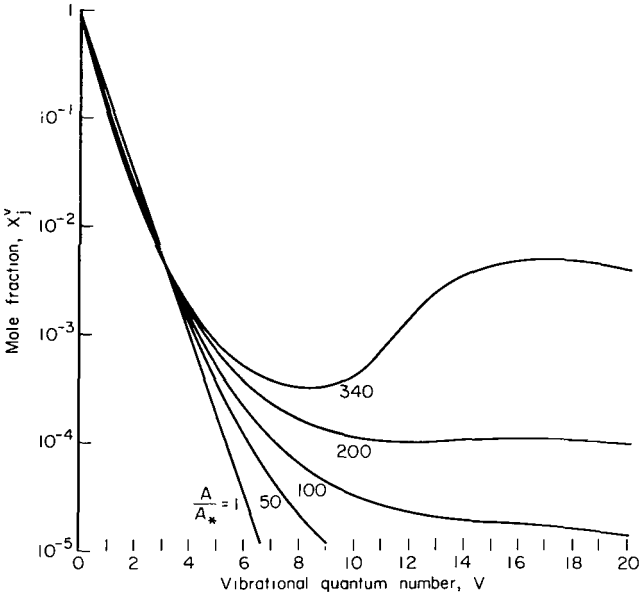

Figure 3.– Population distribution development in CO along the expansion axis. Flow conditions are defined by the standard case described in the text.

Nozzle half-angle	$\phi = 15°$
Nozzle throat height	$h_* = 0.127$ cm
Reservoir temperature	$T_o = 2000°$ K
Reservoir pressure	$p_o = 100$ atm

The nominal transition probabilities referred to throughout this paper are defined by the parameters listed in table 1.

Some resulting characteristics of a single-species solution are illustrated in figures 3 and 4. As expected, the vibrational state populations begin to distort from a near-Boltzmann distribution (represented by a linear plot in fig. 3) as the expansion progresses, and the

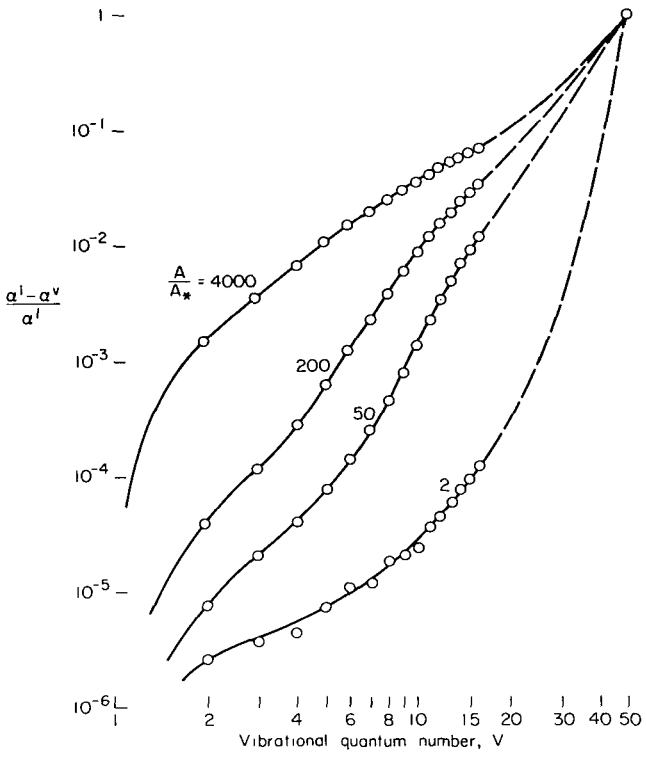

Figure 4.– Solution characteristics for a 16-level CO model.

upper levels finally become overpopulated to the extent that a net inversion develops. This overpopulation is typical (refs. 4, 5) when V - V energy transfer predominates among the lower levels.

In contrast to the behavior of $X_j^v(v,y)$, the variations of the more uniform set, $\alpha_j^v(v,y)$, are shown in figure 4. Their difference fractions from the $v = 1$ value have been computed for the first 16 levels and arbitrarily extrapolated to $\alpha_j^v = 0$ at the dissociation limit. Since α_j^v is an exponential argument, even the small differences shown for the lower levels have a large effect on X_j^v, as evidenced when the constant α distribution plotted in figure 2 is compared to the more exact distributions. There appears to be no simple, low-order polynomial characteristic to the solution, although at this time the waviness of the α_j^v difference curves cannot with certainty be attributed solely to either a solution characteristic or a computational artifact. However, any artificially imposed straightening caused large changes in the corresponding X_j^v distribution, a parameter to which the integration process is also significantly sensitive. The precision of the numerical method is implied by the scatter appearing in the most sensitive data at $A/A_* = 2$. Thus, in view of the straightening effects and apparent stability of the implicit integration scheme, the characteristics as shown in figure 4 are not believed to contain significant numerical errors.

RADIATIVE ASPECTS

The non-Boltzmann character of the population distributions obtained in the preceding calculations may be expected to have some unusual effects on the corresponding radiative properties. Those effects have recently gained importance in the study of vibrationally relaxing flows because, in addition to their influence on the analysis of radiometric measurements, they may be identified as the essential feature that makes gasdynamic laser operation possible in diatomic expansions.

Kuehn and Monson (ref. 16), among others, obtained laser power from the 10.6 μm vibration-rotation bands of CO_2 by placing an optically resonant cavity across the supersonic exhaust of a two-dimensional nozzle. Their results rely on a complete inversion between the lower levels of coupled vibrational modes in a multimode oscillator (viz., CO_2). In the previous section, overpopulation of upper vibrational levels in a single-mode diatomic gas was predicted but a complete inversion was not always achieved. Patel (ref. 17) has shown, however, that a complete vibrational inversion is not necessary for radiative gain in P-branch vibration-rotation transitions, provided the rotational states are sufficiently underpopulated compared to the vibrational states. Such a condition may be characterized by a very low rotational "temperature" in coexistence with a very high vibrational "temperature." Since the non-Boltzmann vibrational distributions previously predicted for carbon monoxide may be represented by very high vibrational temperatures (as determined by the relative population of two adjacent states), and the rapidly relaxing rotational states follow the low kinetic temperatures of the expansion, we may expect to achieve radiative gain within the carbon monoxide vibration-rotation bands, even in the absence of a net inversion.

The Gain Coefficient

Radiative properties for either experimental or laser applications are conveniently described in terms of a small-signal spectral gain coefficient defined by:

$$k(\nu) = \frac{d}{dz} (\ell n\ I_\nu) \tag{22}$$

where z is the optical path coordinate and I_ν is the spectral intensity at frequency ν. Since laser oscillation preferentially seeks the frequency of maximum gain (viz., the line center), and gain measurements are most often made with the contribution of spontaneous emission nullified, the expression for gain coefficient in this application refers only to induced transitions at the line center frequency, ν_o. In terms of the local molecular properties, we can then write

$$k(\nu_o) = N_u h\nu_o B_{u\ell} \eta_{u\ell}(\nu_o) \left(1 - \frac{g_u N_\ell}{g_\ell N_u}\right) \tag{23}$$

where N_u and N_ℓ are the number densities for the upper and lower radiative states, g_u and g_ℓ are their degeneracies, $B_{u\ell}$ is an Einstein coefficient for induced emission, and $\eta_{u\ell}(\nu_o)$ is the corresponding normalized line-shape function, evaluated at the line center frequency, ν_o. For purely Doppler broadened lines, usually considered in most laser applications, Penner (ref. 18) shows that

$$\eta_{u\ell}(\nu_o) = \frac{2}{\Delta\nu_D} \sqrt{\frac{\ell n\ 2}{\pi}} \tag{24}$$

where the Doppler line width is

$$\Delta\nu_D = \frac{2\nu_o}{c}\sqrt{2(\ell n\, 2)\left(\frac{kT}{m}\right)} \tag{25}$$

At most of the gasdynamic conditions to follow, however, collisional broadening also becomes significant, and combined collision and Doppler broadened line profiles, evaluated at the line center, are required. The modified line shape at the line center then becomes

$$\eta_{u\ell}(\nu_o) = \frac{2}{\Delta\nu_D}\sqrt{\frac{\ell n\, 2}{\pi}}\; e^{x^2}\,[1 - \mathrm{erf}(x)] \tag{26}$$

where $x = \sqrt{\ell n\, 2}\;(\Delta\nu_c/\Delta\nu_D)$ and the collision line width for species j is

$$\Delta\nu_c = \frac{1}{\pi}\frac{\rho}{m}\sum_k \hat{X}_k \delta_{jk}\left(\frac{8\pi kT}{\mu_{jk}}\right)^{1/2} \tag{27}$$

Values of average optical cross sections, δ_{jk}, which are assumed to be independent of the rotational state, are listed in table 2 and reference 18 for the gases of interest here.

TABLE 2.- CO RADIATIVE CONSTANTS

B_{10}, $cm^2/erg\ sec$		[a] 6.02×10^5
θ_r, °K		2.778
δ_r		9.05×10^{-3}
δ_{jk}, cm^2	k = CO	5.3×10^{-15}
	k = N_2	5.3×10^{-15}
	K = Ar	1.7×10^{-15}

[a] Based on $A(v,j:v\text{-}1,j\text{-}1) = 1.14\ sec^{-1}$ for $v = 1$; $j = 7$ at $\nu_o = 2169\ cm^{-1}$ (ref. 18).

Equations (23) through (27) may be specialized to the vibration-rotation spectra of a three-dimensional rigid rotor, anharmonic oscillator for vibration-rotation transitions; $u \to \ell = (v, J) \to (v - 1, J \pm 1)$ where v and J are the vibration and rotation quantum numbers. In this case, the Einstein coefficients, $B_{u\ell}$, for degenerate rotation-vibration states with the selection rule, $J = \pm 1$, are correlated by

$$B_{u\ell} = B_{10}v\left(\frac{J + n}{2J + 1}\right) \tag{28}$$

where

$$n = \begin{cases} 0, & \Delta J = -1 \text{ (R-branch)} \\ 1, & \Delta J = +1 \text{ (P-branch)} \end{cases}$$

Since the P-branch gain coefficients are always greater, only $\Delta J = +1$ transitions will be considered further. The molecular constant, B_{10}, is determined from values of the commonly measured Einstein coefficients for spontaneous emission, $A_{u\ell}$, at wavelength $\nu_{u\ell}$ through the relation

$$B_{10} = \frac{c^2}{2h\nu_{u\ell}^3} \frac{A_{u\ell}}{v\left(\frac{J + n}{2J + 1}\right)} \tag{29}$$

The ratio $(g_u/g_\ell)(N_\ell/N_u)$ in equation (23) is evaluated by continuing to assume that the rotational states are populated according to a locally equilibrated Boltzmann distribution defined by the temperature T_r and that $T_r = T$. On that basis, we denote the mole fraction of molecules in the combined rotation-vibration state, v and J, as $X^{v,J}$ and define $X^v = \sum_J X^{v,J}$ which is identical to the vibrational mole fraction, X_j^v, previously computed. If $\Delta E^{v,J}$ is the difference in energy between the Jth rotational state of level v and the ground rotational state of level v, then

$$\frac{X^{v,J}}{g_J} = \frac{X^v \exp\left(\frac{-\Delta E^{v,J}}{kT_r}\right)}{Q_r(T_r)} \tag{30}$$

where $Q_r(T_r)$ is a rotational partition function given by $Q_r = T_r/\theta_r$ and the energy difference is

$$\Delta E^{v,J} = k\theta_r J(J + 1)\left[1 - \delta_r\left(v + \frac{1}{2}\right)\right] \tag{31}$$

In the above, θ_r is a characteristic rotational temperature defined in Herzberg's spectroscopic notation (ref. 19) as $\theta_r = hcB_e/k$ and $\delta_r = \alpha_e/B_e$. The ratio $g_u N_\ell / g_\ell N_u$ for fundamental P-branch transitions is then equal to

$$\frac{g_J X^{v-1,J+1}}{g_{J+1} X^{v,J}} = \frac{X^{v-1}}{X^v} \exp\left[\frac{(\Delta E^{v,J} - \Delta E^{v-1,J+1})}{kT_r}\right] \tag{32}$$

Similarly, the upper level number density in equation (23) may be written

$$N_u = \frac{\rho}{m} (2J + 1) \frac{X^v \theta_r}{T_r} \exp\left(\frac{-\Delta E^{v,J}}{kT_r}\right) \tag{33}$$

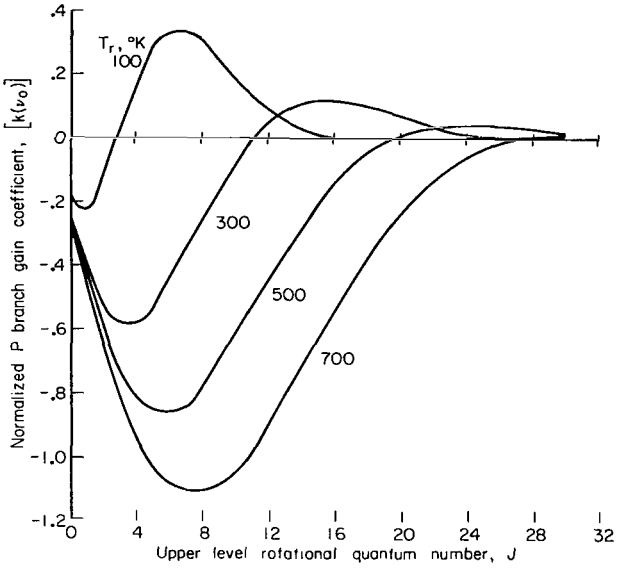

Figure 5.– Normalized CO P-branch gain coefficients for $X^V/X^{V-1} = 0.8$.

The formulation given by equations (23) to (33) is sufficient to compute $k(\nu_o)$ for $\Delta v = 1$ P-branch transitions in terms of ρ, T, and X^V_j from the results of the preceding section. The necessary radiation constants are listed in table 2 for CO.

An example of the results is shown in figure 5 for a gain coefficient assuming only Doppler broadening and normalized by all the factors ahead of the brackets in equation (23) which are independent of J or T_r. Note that the arbitrarily selected population ratio, $X^V/X^{V-1} = 0.8$, does not represent a net inversion; although as T_r decreases, positive gains appear and strengthen. In the calculations to follow, gain coefficients are presented only for the value of J corresponding to the maximum gain in a given vibrational transition.

RESULTS

The brief studies to follow exemplify the features of vibrational relaxation in nozzle expansions that are chiefly an effect of molecular anharmonicity or strongly modified by it. Excellent discussions of the general thermodynamic features of vibrationally relaxing flows may be found in reference 1.

Transition Probability Uncertainties

In the absence of suitable experimental data with adequate sensitivity to the anharmonic effects, we can only indicate the limitations of our numerical results by first evaluating their uncertainty. The uncertainties are contained mainly in the basic vibrational transition probabilities.

Aside from a few exceptions, most vibrational relaxation measurements have provided data pertaining only to the probability of transition between the first and ground states due to V - T exchanges (e.g., refs. 9, 10). A few unique investigations (refs. 11, 12) have provided additional data related to V - V transfer between the two lowest states of dissimilar species, but, in general, no suitable experimental information describing the dependence of probabilities on energy level for either the V - T or V - V cases is known, and very little data is available which defines the magnitude of even the

ground-state V - V rates. Furthermore, all the mechanisms governing relaxation in a practical experimental expansion process are not well understood. For example, some evidence (ref. 20) suggests that residual hydrogen-bearing impurities may cause significant increases in the "effective" V - T relaxation rates. In addition, recent theoretical studies (ref. 21) have demonstrated the importance of previously omitted long-range intermolecular forces at the low temperatures obtained in expansions and the interaction of molecular rotational excitation with the vibrational behavior. The simpler transition probability theories used here therefore contain intrinsic uncertainties of significant magnitudes when applied to an expanding flow, even though the less sensitive shock wave or ultrasonic situations are well described by them.

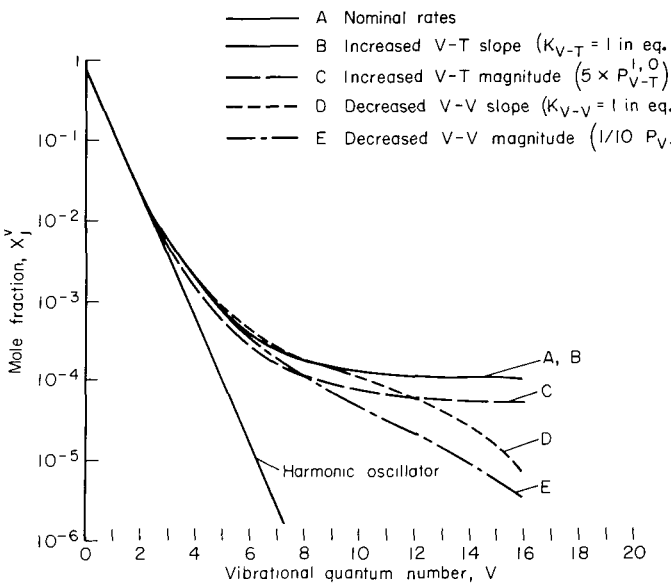

(a) Population distributions.

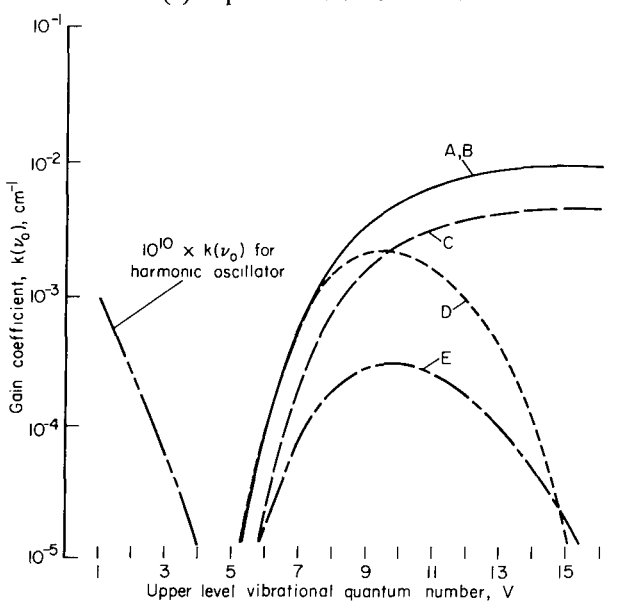

(b) Gain coefficients.

Figure 6.– Probability uncertainty effects for CO at $A/A_* = 200$.

We can show the numerical results to be meaningful, however, if we consider only the gross features of the V - T and V - V probabilities. In the framework of this analysis, those features are described by the ground-state magnitudes $P^{1,0}_{jk}$ and $P_{jk}\binom{1,0}{0,1}$, and the parameter K in equation (9), which controls the slope of the ratios plotted in figure 1. The influence of these parameters on the relaxation process is summarized in figures 6(a) and 6(b), where curves A are based on the nominal values stated earlier. The superimposed curves B are from V - T probability ratios whose increased dependence on v(viz: K = 1) leads to values above the twenty-fifth level greater than 10 times the nominal values. No effect is visible on the lower levels shown and uncertainties of that magnitude will be difficult to resolve. However, a factor of 5

increase in $P_{jk}^{1,0}$ (and thereby in all the V - T probabilities, uniformly) has a measurable effect on all levels (curves C).

Variations in the V - V parameters cause different behavior. A decrease in the probability slope (viz: K = 1, curve D), equivalent to the V - T slope change above, will be observable at levels where the gain is a maximum. Similarly, a factor of 10 reduction in the magnitude of $P_{jk}\binom{1,0}{0,1}$ significantly affects all but the first few levels (curves E).

The nominal $P_{jk}\binom{1,0}{0,1}$ values used here were compared with experimental values reported in reference 12, and were found to overestimate those measurements by a factor of 10. Curves E are therefore adopted as conservative estimates and $(1/10)P_{jk}\binom{1,0}{0,1}$ values are used in the remaining calculations. Since the V - T uncertainties have a smaller effect, their nominal values are retained.

Radiative Gain in CO

The magnitudes of gain given by curves E in figure 6(b) suggest that, even in pure CO, amplification might be sufficient to support laser oscillations in an optical resonator with low losses and sufficient length. (Equivalent loss coefficients are typically 0.01/L or greater where L is the optical path length.) Oscillation would occur preferentially at the ninth to eleventh levels just as found in glow-discharge CO lasers (refs. 17, 22). Other calculations for different gasdynamic conditions indicate that the low gain can be increased by several orders of magnitude by enlarging the throat height to 5 mm, or more. Lesser increases were obtained by halving the expansion angle or doubling the reservoir pressure. Increasing the reservoir temperature did little to increase gain but caused its maximum to shift to higher vibrational levels. All these trends indicate that the flow conditions chosen here as a standard case are, by no means, optimum and appear to be restricting the gain due to excessive freezing of the V - V, as well as the V - T, rate processes.

The radiative gain computed from a harmonic-oscillator model has also been included in figure 6(b). For these conditions, the anharmonicity terms clearly modify the distribution of gain within the vibration-rotation band. Except for predicting radiation from the lowest level, the harmonic-oscillator model is unsuitable for any radiative analysis of this type.

Vibrational Exchange in Mixtures

When a second vibrationally relaxing gas with different relaxation rates and similar energy level spacing is added, vibrational energy is exchanged between the two species and enhances the vibrational excitation of one at the expense of the other. The addition of N_2 to CO expansions has a particularly large influence on the behavior of CO because of two features of N_2: (1) the

vibrational energy levels of N_2 are nearly coincident with those of CO, allowing rapid V - V energy transfer between the two; and (2) the V - T relaxation rates of N_2 are slower than those of CO, allowing N_2 to act as an energy reserve for CO in expansions while making vibrational energy available to CO through V - V collisions. The vibrational "pumping" of CO by N_2 can cause the equivalent CO vibrational temperature to exceed even its initial reservoir temperature. This behavior is illustrated in figure 7 for vibrational temperatures described by the first and ground state populations (see eq. (16)) of each species in several CO-N_2 admixtures.

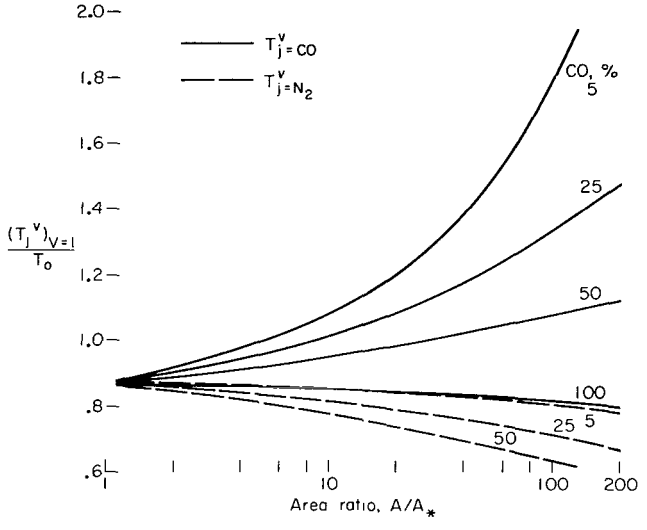

Figure 7.– First level (v = 1) vibrational temperatures in CO-N_2 mixtures. (^{V} – V probabilities are 1/10 the nominal values.)

Others (refs. 4, 23) have shown that if V - V transfer between the two species is rapid compared to the V - T rate, the vibrational states of the two are related by

$$\frac{\theta_{CO}}{(T_{V_{CO}})_{qe}} - \frac{\theta_{N_2}}{(T_{V_{N_2}})_{qe}} = \frac{\theta_{CO} - \theta_{N_2}}{T} \qquad (34)$$

without regard to the anharmonicity of either species. In equation (34), $(T_{V_{CO}})_{qe}$ is the first-level vibrational temperature for a quasi-equilibrium condition maintained under the requirements just described. In expansions of anharmonic oscillators, equation (34) is satisfied initially but becomes less representative as the expansion progresses. A comparison of $T_{V_{CO}}$ obtained from the numerical calculations and from equation (34) using numerical values of $T_{V_{N_2}}$ and T is shown in figure 8. The disagreement that develops between the two is caused by freezing of the V - V process. The later freezing in mixtures of greater CO content is due to the larger V - V probabilities for CO-CO encounters than for CO-N_2 collisions.

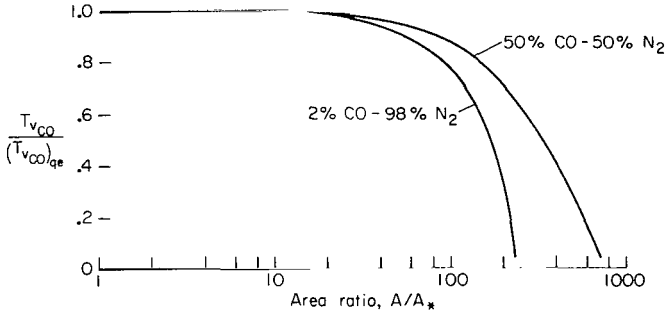

Figure 8.– Deviations from quasi-equilibrium V – V coupling in CO-N_2 mixtures (1/10 P_{V-V}).

Gain Enhancement in Mixtures

The enhancement of CO vibrational excitation caused by V - V exchanges with N_2 also leads to increased gain as figure 9 illustrates. The CO population distribution, in the presence of N_2, becomes more uniform (higher equivalent $T_{V_{CO}}$) and more CO molecules are placed in the upper levels, even though the total number density of CO is reduced. Both factors contribute to increased gain. Figure 9 also indicates that gain is not generally optimized by any single ratio of CO:N_2. The mixture giving maximum gain depends on the vibrational transition of interest as well as the gasdynamic conditions. The general conclusion may be made, however, that the addition of N_2 over a wide range of mixtures raises the CO gain coefficients well above the equivalent optical loss coefficients conveniently obtained in most laser cavities.

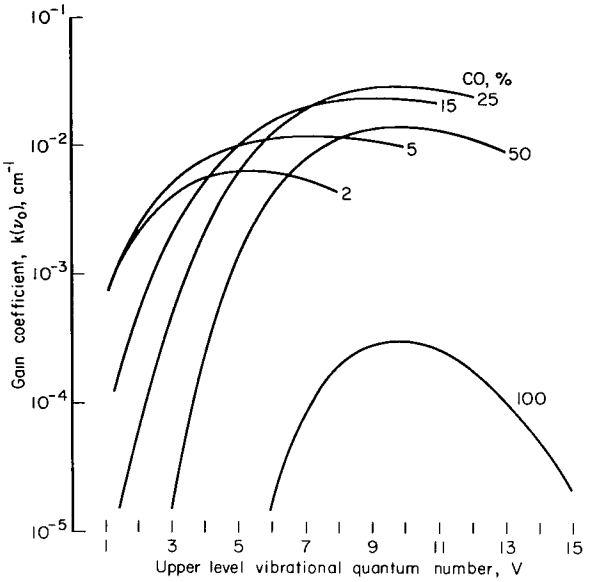

Figure 9.– Gain coefficients in CO-N_2 mixtures at $A/A_* = 200$ $(1/10\, P_{V-V})$.

Gain may be enhanced by other than V - V pumping as well. Figure 5 indicates that gain may also be increased by reducing the rotational temperature. This must be done without affecting the degree of vibrational excitation, however (i.e., without reducing the reservoir temperature). Since rotational relaxation requires only a few collisions, the rotational energy or temperature in most expansions usually remains in thermal equilibrium with the local translational temperature. At a given location in the expansion and from given reservoir conditions, both temperatures may then be reduced through strictly thermodynamic means, by adding large fractions of a monatomic gas. Argon is particularly suitable for this purpose because, as a heavy collision partner, it also reduces the rate of vibrational energy loss through V - T collisions. An example of the net effect is shown in figure 10, where an N_2/CO

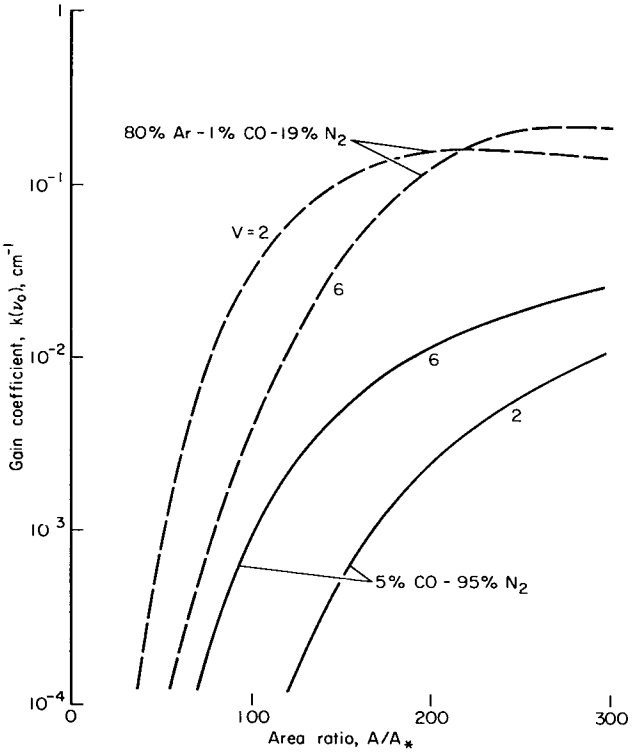

Figure 10.– Gain coefficients in Ar-CO-N_2 mixtures for $\hat{X}_{N_2}/\hat{X}_{CO} = 19$ $(1/10\, P_{V-V})$.

mixture ratio of 1:19 has been diluted with argon. The gain is substantially increased and its maximum is shifted to lower levels.

Diatomic Gasdynamic Lasers

The applications of laser devices depend, in part, on the wavelengths of maximum gain or power. In a diatomic gasdynamic system, the vibrational and rotational level of maximum gain may be shifted downward by going to larger area ratios where the rotational temperature is lower; the gain is increased, and in some nozzles, the optical path is lengthened. This would give rise to laser oscillation at shorter wavelengths with increased power and offer some wavelength selection. Some examples of these variations are shown in figure 11 for an expansion that is limited to $A/A_* = 4000$ by the conditions for condensation of CO to a liquid state. While the lower level gain (v = 1) has reached a maximum determined by the decreasing gas density, higher levels are expected to reach maximum gains limited by other physical properties not included here, particularly gain depletion due to spontaneous radiative decay. In general, the operation of powerful, gasdynamic, diatomic laser devices appears feasible, even in view of the large relaxation rate uncertainties associated with expanding flow predictions.[1]

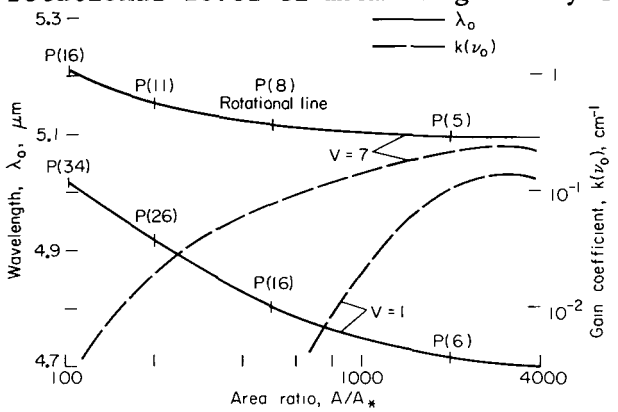

Figure 11.– Wavelength and gain variation along the expansion axis for a 25% CO-75% N_2 mixture ($1/10\ P_{V=V}$).

Ames Research Center
National Aeronautics and Space Administration
Moffett Field, Calif., 94035, October 23, 1970

[1]Since the completion of this theoretical study, the operation of a CO gasdynamic laser based on the principles described here has been demonstrated (ref. 24). Its qualitative behavior is in accordance with these predictions.

REFERENCES

1. Vincenti, Walter G.; and Kruger, Charles H., Jr.: Introduction to Physical Gas Dynamics. John Wiley and Sons, Inc., N. Y., 1965.

2. Hurle, I. R.; Russo, A. L.; and Hall, J. Gordon: Spectroscopic Studies of Vibrational Nonequilibrium in Supersonic Nozzle Flows. J. Chem. Phys., vol. 40, no. 8, April 15, 1964, pp. 2076-2089.

3. Hall, J. G.; and Russo, A. L.: Recent Studies of Nonequilibrium Flows at the Cornell Aeronautical Laboratory. Presented at 7th AGARD Colloquium on Recent Advances in Aerothermochemistry, May, 1966, AGARD Conference Proceedings No. 12, I. Glassman, ed.

4. Treanor, C. E.; Rich, J. W.; and Rehm, R. G.: Vibrational Relaxation of Anharmonic Oscillators with Exchange-Dominated Collisions. J. Chem. Phys., vol. 48, no. 4, Feb. 15, 1968, pp. 1798-1807.

5. Bray, K. N. C.: Vibrational Relaxation of Anharmonic Oscillator Molecules: Relaxation Under Isothermal Conditions. J. Phys. B. (Proc. Phys. Soc.) Ser. 2, vol. 1, no. 4, July 1968, pp. 705-717.

6. Treanor, Charles E.: Vibrational Energy Transfer in High-Energy Collisions. J. Chem. Phys., vol. 43, no. 2, July 15, 1965, pp. 532-538.

7. Schwartz, R. N.; Slawsky, Z. I.; and Herzfeld, K. F.: Calculation of Vibrational Relaxation Times in Gases. J. Chem. Phys., vol. 20, no. 10, Oct. 1952, pp. 1591-1599.

8. Keck, Jame; and Carrier, George: Diffusion Theory of Nonequilibrium Dissociation and Recombination. J. Chem. Phys., vol. 43, no. 7, Oct. 1, 1965, pp. 2284-2298.

9. Millikan, Roger C.; and White, Donald R.: Systematics of Vibrational Relaxation. J. Chem. Phys., vol. 39, no. 12, Dec. 15, 1963, pp. 3209-3213.

10. Hooker, William J.; and Millikan, Roger C.: Shock-Tube Study of Vibrational Relaxation in Carbon Monoxide for the Fundamental and Forst Overtone. J. Chem. Phys., vol. 38, no. 1, Jan. 1, 1963, pp. 214-220.

11. Taylor, R. L.; and Bitterman, S.: Survey of Vibrational Relaxation Data for Processes Important in the CO_2-N_2 Laser System. Res. Rep. 282, Oct. 1967, AVCO Everett Research Laboratory.

12. Taylor, R. L.; Camac, M.; and Feinberg, R. M.: Measurements of Vibration-Vibration Coupling in Gas Mixtures. Proc. Eleventh Symp. (International) on Combustion, Aug. 14-20, 1966, Berkeley, Calif.

13. Treanor, Charles E.: Coupling of Vibration and Dissociation in Gasdynamic Flows. AIAA Paper 65-29, 1965.

14. Bailey, H. E.: Numerical Integration of the Equations Governing the One-Dimensional Flow of a Chemically Reactive Gas. Phys. Fluids, vol. 12, no. 11, Nov. 1969, pp. 2292-2300. Also in Lomax, Harvard; and Bailey, Harry E.: A Critical Analysis of Various Numerical Integration Methods for Computing the Flow of a Gas in Chemical Nonequilibrium. NASA TN D-4109, 1967.

15. Treanor, Charles E.: A Method for the Numerical Integration of Coupled First Order Differential Equations with Greatly Different Time Constants. CAL Rep. AG-1729-A-4, Jan. 1964, Cornell Aero. Lab. Inc.

16. Kuehn, D. M.; and Monson, D. J.: Experiments With a CO_2 Gas Dynamic Laser. Applied Physics Letters, vol. 16, no. 1, Jan. 1, 1970, pp. 48-50.

17. Patel, C. K. N.: Vibrational-Rotational Laser Action in Carbon Monoxide. Phys. Rev., vol. 141, no. 1, Jan. 1966, pp. 71-83.

18. Penner, S. S.: Quantitative Molecular Spectroscopy and Gas Emissivities. Addison-Wesley Pub. Co., Inc., 1959.

19. Herzberg, Gerhard: Molecular Spectra and Molecular Structure, I. Spectra of Diatomic Molecules. D. Van Nostrand Co., Inc., 1950.

20. Von Rosenberg, C. W.; Taylor, R. L.; and Teare, J. D.: Vibrational Relaxation of CO in Nonequilibrium Nozzle Flow. J. Chem. Phys., vol. 48, no. 12, June 15, 1968, pp. 5731-5733.

21. Sharma, R. D.; and Brau, C. A.: Energy Transfer in Near-Resonant Molecular Collisions Due to Long-Range Forces with Application to Transfer of Vibrational Energy from ν_3 Mode of CO_2 to N_2. J. Chem. Phys., vol. 50, no. 2, Jan. 15, 1969, pp. 924-930.

22. Osgood, R. M., Jr.; and Eppers, W. C., Jr.: High Power CO-N_2-He Laser. Appl. Phys. Let., vol. 13, no. 12, Dec. 15, 1968, pp. 409-411.

23. Teare, J. D.; Taylor, R. L.; and Von Rosenberg, C. W., Jr.: Observations of Vibration-Vibration Energy Pumping Between Diatomic Molecules. AMP 268, Oct. 1969, AVCO Everett Res. Lab.

24. McKenzie, Robert L.: 5μm Laser Radiation From a Carbon Monoxide Gasdynamic Expansion. NASA TM X-62,006, 1970. Also in: Applied Physics Letters, vol. 17, no. 10, Nov. 15, 1970, pp. 462-464.

NASA-Langley, 1971 — 12 A-3789

"The aeronautical and space activities of the United States shall be conducted so as to contribute . . . to the expansion of human knowledge of phenomena in the atmosphere and space. The Administration shall provide for the widest practicable and appropriate dissemination of information concerning its activities and the results thereof."

—NATIONAL AERONAUTICS AND SPACE ACT OF 1958

NASA SCIENTIFIC AND TECHNICAL PUBLICATIONS

TECHNICAL REPORTS: Scientific and technical information considered important, complete, and a lasting contribution to existing knowledge.

TECHNICAL NOTES: Information less broad in scope but nevertheless of importance as a contribution to existing knowledge.

TECHNICAL MEMORANDUMS: Information receiving limited distribution because of preliminary data, security classification, or other reasons.

CONTRACTOR REPORTS: Scientific and technical information generated under a NASA contract or grant and considered an important contribution to existing knowledge.

TECHNICAL TRANSLATIONS: Information published in a foreign language considered to merit NASA distribution in English.

SPECIAL PUBLICATIONS: Information derived from or of value to NASA activities. Publications include conference proceedings, monographs, data compilations, handbooks, sourcebooks, and special bibliographies.

TECHNOLOGY UTILIZATION PUBLICATIONS: Information on technology used by NASA that may be of particular interest in commercial and other non-aerospace applications. Publications include Tech Briefs, Technology Utilization Reports and Technology Surveys.

Details on the availability of these publications may be obtained from:

SCIENTIFIC AND TECHNICAL INFORMATION OFFICE

NATIONAL AERONAUTICS AND SPACE ADMINISTRATION

Washington, D.C. 20546